Development of a miniature fan motor

Chien-Chang Wang, Yeong-Der Yao, Kun-Yi Liang, Chung-Chun Huang, and Yu-Choung Chang

Citation: Journal of Applied Physics **111**, 07E718 (2012); doi: 10.1063/1.3675993
View online: http://dx.doi.org/10.1063/1.3675993
View Table of Contents: http://scitation.aip.org/content/aip/journal/jap/111/7?ver=pdfcov
Published by the AIP Publishing

Development of a miniature fan motor

Chien-Chang Wang,[1,a)] Yeong-Der Yao,[2,3] Kun-Yi Liang,[1] Chung-Chun Huang,[1] and Yu-Choung Chang[1]
[1]*Green Energy and Environment Research Laboratories, Industrial Technology Research Institute, Hsinchu, Taiwan*
[2]*Department of Materials Science and Engineering, National Chiao Tung University, Hsinchu, Taiwan*
[3]*Department of Physics and Institute of Applied Science and Engineering, Fu Jen University, Taipei 242, Taiwan*

(Presented 1 November 2011; received 23 September 2011; accepted 8 November 2011; published online 2 March 2012)

A novel compact axial flux fan motor was developed. Such a micromotor could be a potential candidate for using as the cooling solution for the next generation mobile devices, for example, smart phones and pico-projectors. The key parameters of the motor, such as back electromotive force, cogging torque, and axial preload are predicted using finite element method. In addition, new approaches are proposed to measure these items, and the corresponding experimental results are in good agreement with the simulated one. Moreover, the undesired vibration harmonic is successfully suppressed, and the fan motor represents a high static pressure and air flow rate. © *2012 American Institute of Physics*. [doi:10.1063/1.3675993]

I. INTRODUCTION

More and more consumer electronic products, for example, smart phones and pico-projectors are becoming an increasing demand in our daily life to make our communication and information sharing easier and faster. The design characteristics of these devices are the requirement for light, thin, small, and multifunction in order to fulfill the need of end user, and these specialized features result in the thermal problems. Therefore, the increasing demand of cooling approach for the portable devices is worthy to be studied. In fact, a pico-projector in which display panel, LED source, IC chips, and battery contribute the dominant heat to the system, and active cooling must be employed in order to attain the sufficient low temperature such that the projecting brightness can be maintained. Walsh *et al.*[1] investigated the cooling performance of a tiny fan implemented into a mobile phone. Focused upon the cooling issue for the handheld electronic devices, this research aims to develop a new miniaturized single-phase blushless fan motor. In order to reach the compact size, the axial flux type motor[2] was adopted. 3D finite element method (FEM) was used to simulate the parameters of the motor, such as torque constant (*kt*), output torque (*T*out), cogging torque,[3] and axial preload. In addition, a brand new technique using a contactless driving to detect the *kt* for the small motor was disclosed. Moreover, a method utilizing the adjustment of phase angle between the *T*out and cogging torque was proposed to decrease the magnitude of the undesired axial vibration harmonic. When analyzing the phase effect for the output torque harmonics, the variable *T*out is equivalent to the sum of *T*out and cogging torque.

II. DESIGN OF A MINIATURE AXIAL FLUX MOTOR

Figure 1 shows the structure of the proposed motor, and the main parameters of the motor can be referred to Table I. A cheap sleeve bearing, which makes the manufacture price more competitive, is employed. The PM is made of high energy product neodymium-iron-boron (NdFeB) with a residual flux density of 5630 G, and a magnetic sheet (MS) is introduced for enhancing the capacity of output power. The rotational speed of the micro motor is 6500 rpm. The 3D FEM model for solving the parameters of the proposed motor in which 881 632 tetrahedral elements are assigned. Maxwell stress tensor method (MSTM)[3] is used to estimate *kt*, *T*out, cogging torque, and axial preload. One degree of mechanical angle increment per sample for solving above parameters is decided in the simulation processes, and the estimation is performed until one periodic rotation of 120 deg (mechanical angle) is computed. On the other hand, the back electromotive force (Back-EMF) constant (*ke*) can be determined by means of calculating the flux linkage (FL) of the coils[3] and compared with the torque constant for validating the simulation results.

Figure 2(a) shows the simulated *kt* and *ke* compared with the measured *ke*. The peak values for the former and

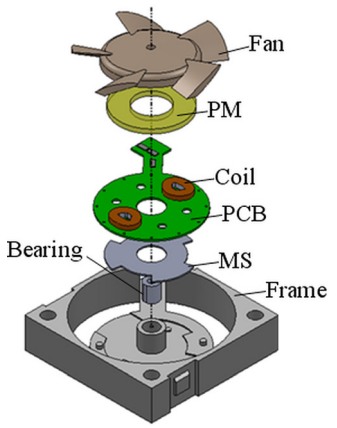

FIG. 1. (Color online) Structure of the compact fan motor.

a)Electronic mail: JamesCCW@itri.org.tw.

TABLE I. Parameters of the proposed motor.

Parameter	Unit	Value
Rated voltage	V	3.3
Operating current	mA	<25
Diameter	mm	9
Height	mm	3.47
Axial air gap	mm	0.3
Pole number	-	6
Slot number	-	2

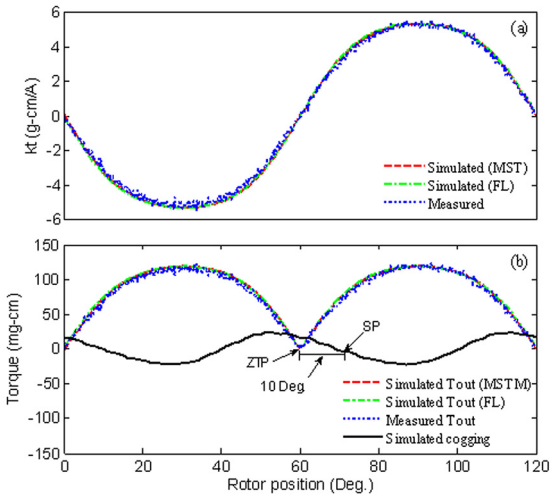

FIG. 2. (Color online) 3D FEM simulation results for the developed motor. (a) Torque constant curves. (b) Torques.

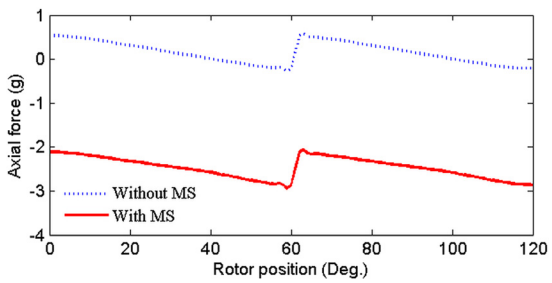

FIG. 3. (Color online) Simulated axial force profiles for motor with and without MS.

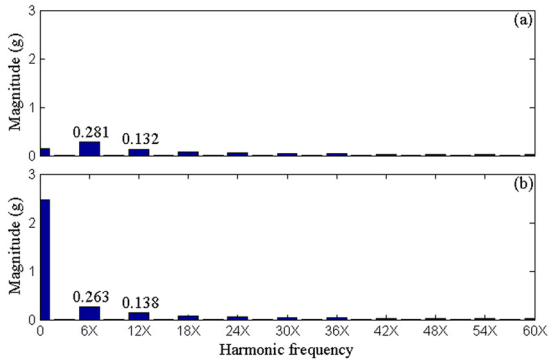

FIG. 4. (Color online) Simulated frequency spectra of axial preload. (a) Without MS. (b) With MS.

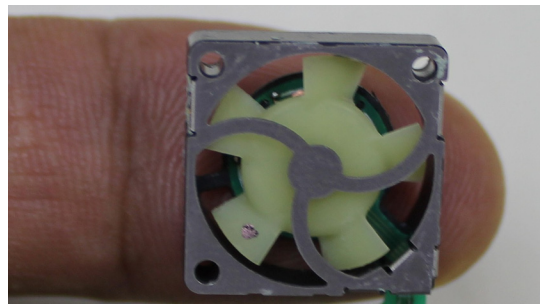

FIG. 5. (Color online) Mock-up of the prototyped fan motor.

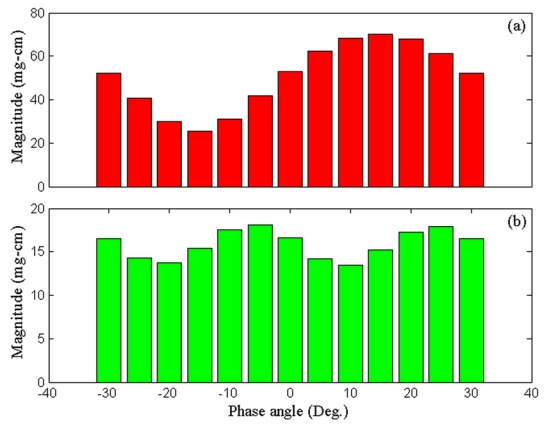

FIG. 6. (Color online) The effect of lead-lag phase angle for 6*X* and 12*X* output torque harmonics. (a) 6*X*. (b) 12*X*.

latter are 5.331, 5.330, and 5.532 g-cm/A, respectively. The curves indicate that the distributions of *kt* and *ke* predicted by FEM match the experimental data very well. Since the units of *kt* and *ke* in MKS unit are equivalent, the *ke* is represented in terms of g-cm/A. Utilizing the *kt* multiplied by the exciting current of the motor the output torque can be obtained, as shown in Fig. 2(b). Pointed out in the Fig. 2(b), the stable point (ST) of the cogging lags 10 deg behind the zero-torque point (ZTP), apparently, when the rotor intrinsically stop at the SP, the design can avoid the problem of starting dead-point[4] of the motor because the *T*out is greater than the cogging. Figure 3 shows the simulated axial preload versus rotor position. Because the axial preload profile has a period of 120°, the fast Fourier transformation was used to

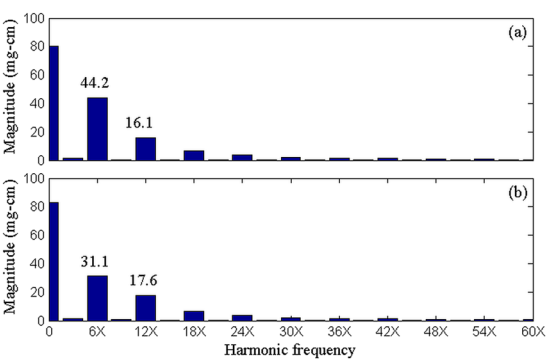

FIG. 7. (Color online) Simulated frequency spectra of the output torque. (a) Without MS. (b) With MS.

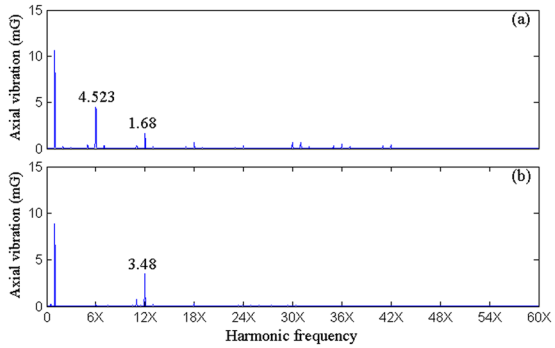

FIG. 8. (Color online) Measured frequency spectra of the axial vibration. (a) Without MS. (b) With MS.

determine the magnitudes of the harmonic components, and the corresponding frequency spectra are shown in Fig. 4. The peak value for the magnitude of simulated axial preload (With MS) is 2.939 g, which is close to the measured quantity of 2.738 g. Comparing the Figs. 4(a) and 4(b), it is manifest that the axial preload does not contribute to neither the magnitude of 6*X* axial vibration harmonic nor the 12*X* where *X* designates the rotational frequency of the motor because the variation of the above two magnitudes in both conditions of before and after the removal of MS can be ignored.

III. MOCK-UP AND EXPERIMENT

Figure 5 shows the mock-up of the proposed fan motor. For being as a cooling solution of the next generation of mobile devices, the blade which was designed with maximized maximum static pressure (*P*) and maximum volumetric flow rate (*Q*) was supported by S. C. Lin's Lab in National Taiwan University of Science and Technology. The frame size of the mock-up is 16 mm long by 16 mm width by 4 mm height. The *P-Q* testing system consisting of three major elements a Laminar flow element (Meriam model 50MJ10) and two pressure transmitters (Rosemount model 3051) was assembled. While measuring *P-Q* curve, the aided fan was driving the tested fan, mounted on the other side of the system, via the wind tunnel without any contact. Meanwhile, *DP* and *Ps* transmitters were transferring the signals to the data recorder, and then the *P* and *Q* information was collected. Obviously, the rotational speed of the fan was gathered by the RPM meter. The measured *P-Q* curve of the fan at the speed of 6500 rpm shows that the maximum value for *P* and *Q* are 0.424 *mmAq* and 0.164 *CFM*, respectively. In general, conventional method[2] used double-sided axial flux type motor to measure the EMF; however, the additional stator coil must be added. Using the same testing system, the fan was driven to various steady speeds, and then the back-EMF was obtained by an oscilloscope at different rotational speeds. Thus, the *ke* can be successfully obtained.

IV. RESULTS AND DISCUSSION

Figure 6 displays the simulated magnitude of 6*X* *T*out harmonic [see Fig. 6(a)] and the 12*X* [See Fig. 6(b)] affected by the lead-lag phase angle which is the angle between the SP and ZTP. The effect was observed when the angle was in the range of $-30°$ to $30°$. Clearly, the minimized 6*X* magnitude occurs at $-15°$; however, the phase angle of $-10°$ is selected as prototyping the motor in that the mechanical layout constraints of PCB, driver IC chip, and the coils. While the fluctuation of the magnitude of 6*X* is significantly related to the change of the phase angle, the 12*X* is not. Finally, the decline in magnitude of 6*X* of the prototyped motor, as compared with the motor inside which the MS is not embedded, is up to 29%, i.e. the shifting phase angle can sharply suppress the magnitude of 6*X* axial vibration harmonic in comparing with the motor without the MS. As shown in Fig. 7(a) the magnitude of 6*X* *T*out harmonic and the 12*X* for the motor without MS are 44.2 and 16.1 mg-cm, respectively. As is well known, human hands are sensitive to the vibration if its frequency lies in the interval from around 200 to 800 Hz, this is the reason why the reduction of 6*X* magnitude is the most concerned. Eventually, Fig. 8 shows the experimental results for the axial vibration of the mock-up motor. As the motor is not equipped with a MS, the magnitude of the 6*X* is 4.523 mG (1 G = 9.8 m/s^2); however, after the MS is installed, the magnitude is apparently eliminated. In short, the analysis of the simulated *T*out and measured axial vibration frequency spectra tells that the magnitude of the 6*X* axial vibration harmonic is dominated by pulsated output torque. Contrary to expectation, the 12*X* is abnormally increased as the MS is installed, and the continuing work will be focused on this problem in the future.

V. CONCLUSIONS

A thumb-sized fan motor has been developed. It can create a maximum static pressure of 0.424 *mmAq* and a maximum volumetric flow rate of 0.164 CFM. In addition, the lead-lag phase adjustment method shifting the phase angle between the stable point of cogging torque and zero-torque point of output torque can effectively eliminate the magnitude of the undesired 6*X* (648 Hz) axial vibration harmonic, which is dominated by the pulsated output torque, after the MS is installed. Furthermore, aerodynamic flow of air used to drive the tested fan through the wind tunnel was proposed to measure the key parameter back-EMF constant for such a tiny motor. And, the measured EMF constant matches simulation result very well. This research successfully demonstrated a potential fan motor to be expected to contribute to the active cooling for the next generation portable devices.

[1]R. Grimes, E. Walsh, and P. Walsh, Appl. Therm. Eng. **30**, 2363 (2010).
[2]N. Achotte, P. A. Gilles, O. Cugat, J. Delamare, P. Gaud, and C. Dieppedale, J. Microlelctromech. Syst. **15**, 1001 (2006).
[3]Y. D. Yao, D. R. Huang, J. C. Wang, S. H. Liou, S. J. Wang, T. F. Ying, and D. Y. Chiang, IEEE Trans. Magn. **33**, 4095 (1997).
[4]C. M. Chao, S. J. Wang, C. P. Liao, D. R. Huang, and T. F. Ying, IEEE Trans. Magn. **34**, 471 (1998).